DOI: 10.1002/ejic.200800585

Synthesis and Characterization of a (Dipyridylthiophene)platin Complex of a Pyridyl-Substituted Aminoethylglycine Artificial Dipeptide

Lauren A. Levine,[a] Hye Won Youm,[a] Hemant P. Yennawar,[a] and Mary Elizabeth Williams*[a]

Keywords: Platinum / Heterocycles / Luminescence / Peptides

We report the solution-phase synthesis and characterization of an artificial pyridyl-substituted dipeptide that is crosslinked by a 2,5-bis(2-pyridyl)thiophene (dpt) platinum complex. The small molecule equivalent for the Pt(dpt)dipyridyl-peptide is synthesized for comparison. These compounds are characterized by two-dimensional and variable-temperature NMR, mass spectrometry, electrochemistry, UV/Vis absorbance and emission spectroscopy, and their photoemission dynamics are compared. The complexes have two reversible, ligand-centered reductions, are luminescent at room temperature, and have two distinct radiative relaxations with nanosecond and microsecond lifetimes. These metallated peptide building blocks are promising for use as stable inorganic complexes to label synthetic peptides with luminescent and redox-active probes.

Introduction

Artificial oligopeptides containing metal-coordinating ligands on an aminoethylglycine (aeg) backbone have been designed for use as nucleic acid sensors,[1] molecular wires,[2] stabilizers for PNA–PNA[3] and PNA–DNA[4] interactions, and artificial photosynthetic centers.[5] It has been shown that the pendant ligands stoichiometrically coordinate metal ions and complexes are held at distances that are defined by the spacing of substituents along the backbone. Artificial peptides have been incorporated into peptide nucleic acid (PNA) strands,[3,4] glycerol nucleic acids (GNA),[6] and in completely artificial architectures.[1a,2,5] Among these previously reported systems, there has been a limited number of luminescent metal-ligand complexes that have been installed[1b,5,7] and could be employed as fluorescent tags in biological systems or for photoinduced electron and energy transfer in multi-metallic architectures. An ongoing challenge for artificial peptides is to exert control over the relative placement and assembly of heterometallic species in these architectures. Using substitutionally inert transition metal complexes, it is feasible to employ metallated peptide monomers or dimers as building blocks during peptide synthesis. We have therefore sought a route to prepare stable, inert inorganic complexes on an artificial peptide scaffold that could further be used as emissive tags for the host of envisioned biological and photophysical applications. Synthetic modification of the ligand(s) that coordinate Pt^{2+} has led to the design of complexes with long-lived excited state lifetimes and high-emission quantum yields in solutions at room temperature. The photophysical properties of these complexes would be useful for many of the potential applications, making these attractive candidates for incorporation into the artificial oligopeptide library.

One strategy pioneered by von Zelewsky[8] and others[9] is the formation of a carbon–Pt bond through the chelation of a 2-arylpyridine ligand. The resulting complexes have high quantum yields that range from 0.14–0.35 and microsecond excited state lifetimes.[9c,9d,10] These Pt^{II} complexes have been used in light-emitting devices (OLEDs),[11] catalysts in the photogeneration of hydrogen,[12] singlet-oxygen sensitizers,[9f,13] photovoltaic devices,[14] and biological sensors.[9d,15] Adjustment of the relative energies of the metal-to-ligand charge-transfer band (MLCT) and non-emissive metal-centered band (MC) is accomplished by variation of the degree of saturation and substitution of the ligands. Although there are a few examples of synthetic modifications to the 2-(2′-thienyl)pyridine (thpy) family of the 2-arylpyridine ligands, these have been limited to fused benzyl rings,[9c,9e,9f] methyl/methoxy groups,[9e] and conversion to a tridentate ligand by addition of a phenyl ring.[9d,16] In all cases the planarity of the heterocyclic ligand system is maintained because it plays a role in the excited-state energetics that enable these species to be highly emissive.

A family of Pt(thpy) complexes with varying ligands, including diimine (saturated and unsaturated), dithiolate, diphosphinate, or diketonate complexes, illustrates the tunability of the spectroscopic and electrochemical properties. Excited-state relaxation by photoemission occurs by relax-

[a] Department of Chemistry, The Pennsylvania State University, 104 Chemistry Building, University Park, Pennsylvania, PA 16802, USA
E-mail: mbw@chem.psu.edu

Supporting information for this article is available on the WWW under http://www.eurjic.org or from the author.

ation from the π* states on the diimine in complexes with unsaturated ligands; in contrast, with saturated diimine ligands the emissive state is assigned to a ^{3}LC transition from the cyclometalate.[9c,10b] Variation of both the ligand bound to the Pt(cyclometalate) and its substituents alters the electrochemical properties of these molecules.

We have previously described the synthesis and characterization of artificial oligopeptides with an aminoethylglycine (aeg) backbone that contain heterocyclic pendant ligands.[2,5] These compounds rely on metal coordination to form the single-stranded,[2a,2b] duplex,[2a,2c,2d] and hairpin[5] geometries shown in Scheme 1. These structures self-assemble on the basis of the denticity of the attached ligand and coordination chemistry of the added metal ions. We report here the solution-phase synthesis and characterization of an artificial dipyridyl aeg dipeptide [Boc-(py-aeg)$_2$-OEt] in which the two pyridine ligands both coordinate to a single [Pt(2,5-bis(2-pyridyl)thiophene)]$^{1+}$ (dpt) complex. The small molecule equivalent containing two picoline ligands coordinated to [Pt(dpt)]$^{1+}$ was synthesized for comparison of the structural and physical properties. Both [Pt(dpt)x$_2$]$^{1+}$ (x is py-aeg or picoline) complexes emit light following photoexcitation at room temperature, and have two distinct radiative transitions with nanosecond and microsecond lifetimes. Because the aeg scaffold is amenable for incorporation into peptide strands by amide coupling chemistry, the [Pt(dpt)(py-aeg)$_2$] dipeptide has potential use as a metallated artificial amino acid for labeling modified peptides with a fluorescent and redox active probe.

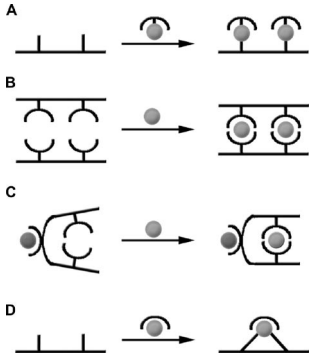

Scheme 1. Metal coordination to artificial peptides: (A) metallated single strands; (B) metal-induced duplex formation; (C) metal induced hairpin formation; (D) intrastrand crosslinks.

Results and Discussion

Dipeptide Synthesis

Our group has used solid-phase peptide synthesis to prepare artificial aeg peptides by efficient separation of peptide-coupling reagents from the oligomers.[2a,2b,2d] However, we have been limited by the small quantities that are afforded by solid-phase synthesis, which is largely determined by the loading of functional groups on the resin support.[2a,2b,2d] To increase the quantities of material that are available for electrochemical and spectroscopic investigations, we have recently turned to purely solution-phase peptide syntheses. To accomplish these, in this work the protecting groups on the ligand-modified aeg monomers have been slightly modified: the pyridine monomer [Boc-(py-aeg)-OEt] was prepared with the two different protecting groups of a base-labile ethyl ester and acid-labile Boc derivative. In separate reactions, the terminal acid was deprotected in 65% yield, and the Boc cleaved from amine terminus in 75.4% yield.

The deprotected monomers were used to synthesize the pyridine-substituted dipeptide Boc-(py-aeg)$_2$-OEt as shown in Scheme 2, which was purified by column chromatography.

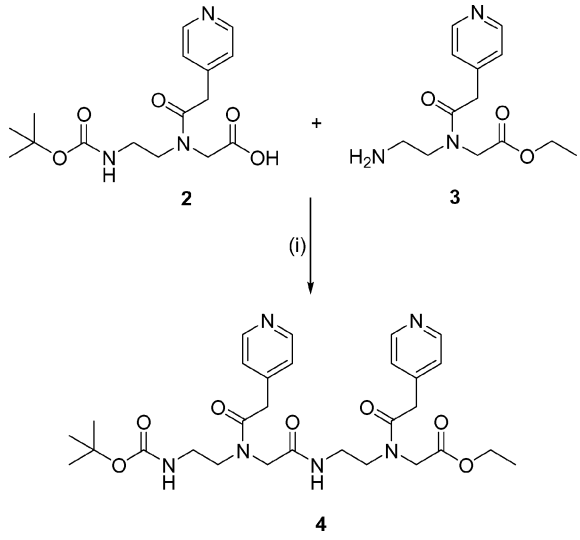

Scheme 2. Synthesis of the Boc-(py-aeg)$_2$-OEt (**4**): (i) **2** w/HBTU, HOBt, DIPEA, DCM/1 h 0 °C, addition of **3** DCM/3 d room temperature follow with column (35% yield).

In comparison with our previous report of artificial pyridyl aeg peptides,[2b] this dipeptide was prepared in higher yield (34.8% vs. 29% by solid-phase synthesis) and in much larger scale (590 mg vs. 43 mg by solid phase). To confirm the identity and purity of the dipeptide, analysis by electrospray ionization mass spectrometry (ESI+ MS) and ^{1}H NMR was performed. The aromatic region of ^{1}H NMR spectrum (Supporting Information) is simplified compared to that of our previously reported py-aeg oligopeptides, which contained a benzoyl terminal group at the N-terminus. The aliphatic region of the spectrum is still complicated by the presence of rotational conformers, however comparison of the peak areas for the aromatic and aliphatic regions confirms the purity of the dipeptide. Mass spectrometry reveals the molecular ion peak, further verifying the identity of the desired Boc-(py-aeg)$_2$-OEt.

Reactions with Pt(dpt)

Previously, pyridyl-substituted aeg oligopeptides were employed for Cu^{2+} and Pt^{2+} metal coordination.[2a–2b,17] Adapting the straightforward approach of Lowe et al.,[18] we used the method in Scheme 3 to react [Pt(cyclooctadi-

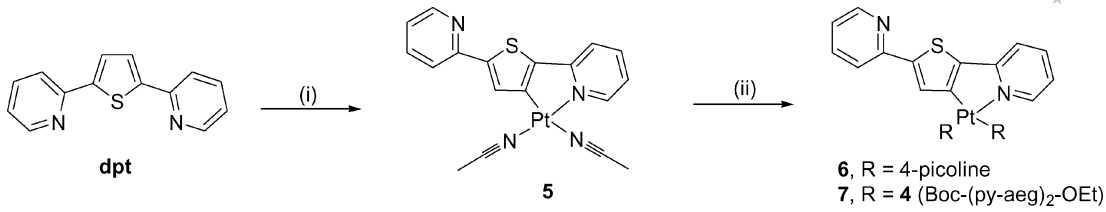

Scheme 3. Synthesis of Pt(dpt) complexes. (i) $Pt(cod)ClO_4$ acetone/acetonitrile (2:1) reflux overnight; (ii) 4-picoline (yield 61%)/Boc-(py-aeg)$_2$-OEt (yield 44.5%) ACN/room temp., 2 d.

ene)ClO_4] with the dpt ligand in acetonitrile to give the $[Pt(dpt)(ACN)_2]^{1+}$ complex. Reaction of this with pyridine-based ligands causes disassociation of the ACN; complexes **6**–**7** (Figure 1) were obtained in good yields (44–61%) following purification by column chromatography.

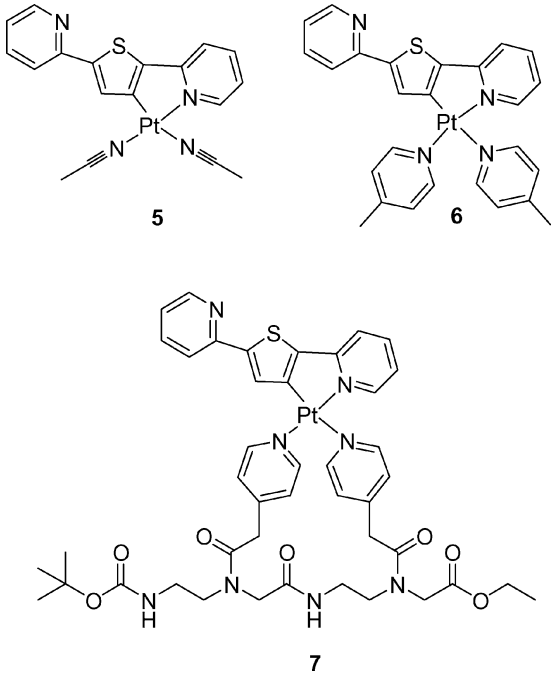

Figure 1. Pt(dpt)-containing complexes prepared in this study.

The identity of the compounds was determined by time-of-flight positive ion electrospray (TOF-ES+) mass spectrometry. In each case, the mass spectra of **6**–**7** contained the molecular ion peaks of the expected product, and the purity of the products was confirmed using ^1H NMR spectroscopy. (Supporting Information)

Crystal Structures

Single crystals of the dpt ligand and $[Pt(dpt)(4\text{-pic})_2]^{1+}$ complex (**6**) were grown from acetonitrile/acetone solutions by slow evaporation of solvent at room temperature, and characterized using X-ray crystallography. The crystal structures of each of these are shown in Figure 2 and selected bond lengths and angles are collected in Table 1. The structure of the dpt ligand is planar with slight distortion along one of the pyridyl rings and a torsion angle of –8.6(2)° for N1–C5–C6–S1 and 3.11(18)° for S1–C9–C10–N2. The bond angles and lengths for the dpt ligand are similar to those reported for related thpy ligands.[19]

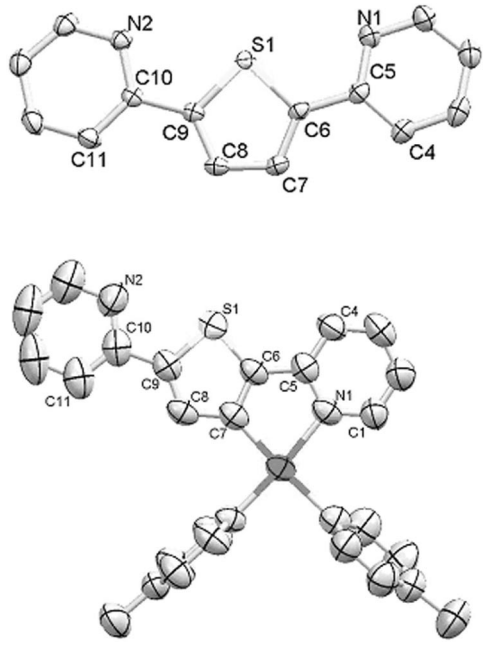

Figure 2. X-ray single crystal structure of (top) the dpt ligand and (bottom) Pt complex **6**. Thermal ellipsoid at 50% probability, hydrogen atoms and perchlorate counterions are omitted for clarity.

Complexation of Pt does not distort the planarity of the dpt ligand [torsion angles of 0° for C4–C5–C6–S1 and 3.6(9)° for S1–C9–C8–N2], as shown in Figure 2. The crystal structure reveals that the dpt ligand coordinates the Pt in a bidentate fashion by formation of one nitrogen–Pt bond and one carbon–Pt bond, the latter of which is characteristic of the Pt(thpy) family of compounds. The coordination geometry around the Pt is slightly distorted square planar with no observed metal–metal interactions (Pt–Pt distance 5.026 Å). The C(7)–Pt(1) [1.968(8) Å] bond length is similar to values reported in other Pt(thpy) complexes (1.989(6) to 1.953(7) Å[9c,9e]]; whereas the N(1)–Pt(1) [2.056(6) Å], N(3)–Pt(1) [2.015(6) Å], and N(4)–Pt(1) [2.111(7) Å] bond lengths are slightly larger or comparable to values from other Pt(thpy) complexes in which the other ligand has a weak trans influence.[20] Likewise, there are marked similarities in the bond angles in **6** vs. other Pt(thpy) complexes: the N(1)–Pt–C(7) angle of 81.0(3)° is analogous to the mean angle of 80.7° for cyclometalated Pt^{II} complexes.[21]

Table 1. Selected bond lengths [Å] and angles [°] for dpt and **6**.

	dpt	6
C(4)–C(5)	1.401(2)	1.350(10)
C(5)–N(1)	1.344(2)	1.383(9)
C(5)–C(6)	1.464(2)	1.434(10)
C(6)–C(7)	1.373(2)	1.366(9)
C(6)–S(1)	1.7285(17)	1.731(7)
C(9)–C(10)	1.467(2)	1.487(11)
C(9)–S(1)	1.7274(17)	1.728(7)
C(10)–N(2)	1.345(2)	1.359(12)
C(10)–C(11)	1.393(2)	1.375(12)
C(7)–Pt(1)	–	1.968(8)
N(1)–Pt(1)	–	2.056(6)
N(3)–Pt(1)	–	2.015(6)
N(4)–Pt(1)	–	2.112(7)
N(1)–C(5)–C(6)	116.26(15)	113.4(6)
C(4)–C(5)–C(6)	121.64(17)	126.9(7)
C(7)–C(6)–C(5)	128.98(15)	118.2(7)
C(10)–C(9)–S(1)	120.00(13)	127.9(5)
N(2)–C(10)–C(9)	116.44(16)	115.2(9)
C(11)–C(10)–C(9)	121.19(15)	121.4(9)
C(7)–Pt(1)–N(1)	–	81.0(3)
C(7)–Pt(1)–N(3)	–	93.5(3)
N(3)–Pt(1)–N(4)	–	91.0(2)
N(1)–Pt(1)–N(4)	–	94.5(3)

NMR Spectroscopy

Assignments for each of the proton and carbon shifts in the NMR spectra for **6** were determined by analysis of the data from both 1D experiments and COSY, HMQC and HMBC spectra (see Supporting Information). On the basis of the analysis of all of these data, the peak positions in the spectrum (Figure 3) for **6** indicate an upfield shift for the protons in the *meta*-position (**M**, **K**, **I** and **G**) and a downfield shift for the *para*-position protons (**L** and **H**) (see Figure 3 inset for structure labels). In contrast, there is an upfield shift of about 0.6 ppm (vs. the free ligand) for the *ortho*-protons (**N** and **F**). The shifts on the terminal pyridyl-ring of the dpt are shifted downfield due to the deshielding effect of the Pt bound thiophene-pyridyl complex. Similar downfield shifts are observed for the picoline ligand protons.

The chemical shifts in the ^{1}H NMR spectrum of **7** are broadened relative to those for **6**, however the spectra of **7** can be interpreted aided by the assignments from the small molecule analog and the COSY and HMQC experiments. In the case of **7**, coordination of the Pt complex forces the pyridyl ligands into a more rigid conformation; broadening and rotational conformers are therefore observed in both the aliphatic and aromatic regions of the spectrum. When the sample is heated, coalescence of the peaks occurs but broadening is still visible as seen in the series of ^{1}H NMR spectra taken at the indicated temperatures in Figure 4. This experiment demonstrates that even at the highest temperatures, the rate of exchange is still on a slow enough time scale that the peaks have not completely coalesced.

Consistent with prior studies of pyridine-substituted oligopeptides[2,22] and PNA[23] structures, rotational conformers complicate the aromatic and aliphatic regions of ^{1}H NMR spectra. In this case, the spectrum is further complicated by the increased number of chemically non-equivalent protons that are created upon binding of Pt(dpt) to the dipeptide; the combination of conformers and chemically non-equivalent protons makes the assignment of the aliphatic region difficult. Nonetheless, by identifying the protons from the protecting groups at elevated temperature, the relative integrations of the peaks in the aromatic and aliphatic regions are quantitatively compared. This reveals the expected relative number of protons in these regions, further confirming the identity and purity of complex **7**. In the ^{13}C NMR spectra, similar shifts in the carbon peaks are exhibited by both **6** and **7**, as shown in the HMQC spectra in Figure 5. The spectrum of **7** has negligible shifts compared to the unmetallated dpt ligand for the unbound pyridyl ligand ($\Delta\delta$ = 0.2–3.2 ppm).

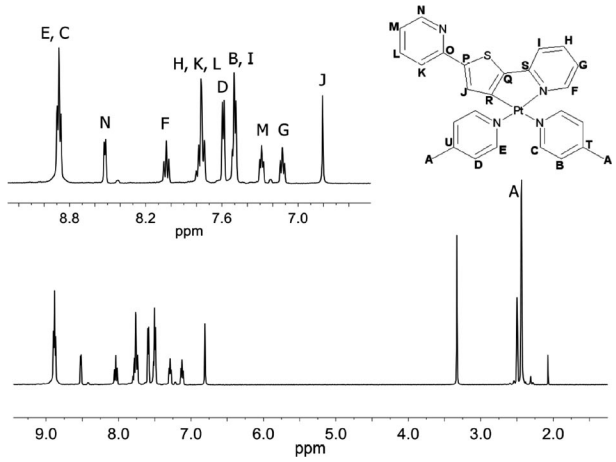

Figure 3. ^{1}H NMR (400 MHz) spectra of **6** in [D_6]DMSO and (Inset) expansion of the aromatic region.

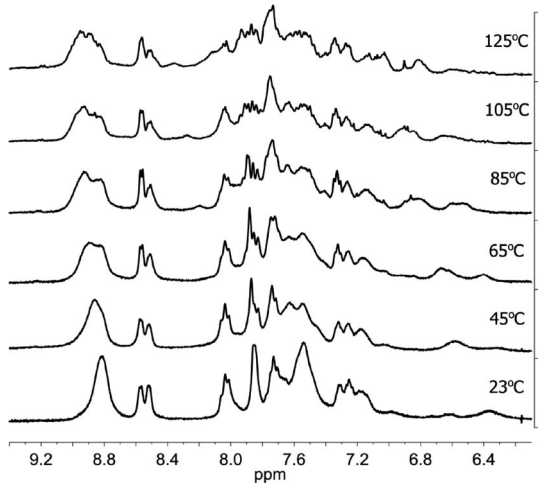

Figure 4. ^{1}H NMR (300 MHz) spectra of **7** in [D_6]DMSO acquired at the indicated temperatures.

Electrochemistry

Application of cathodic potentials induces a ligand-centered reduction of the heteroaromatic ligands in the Pt^{2+}

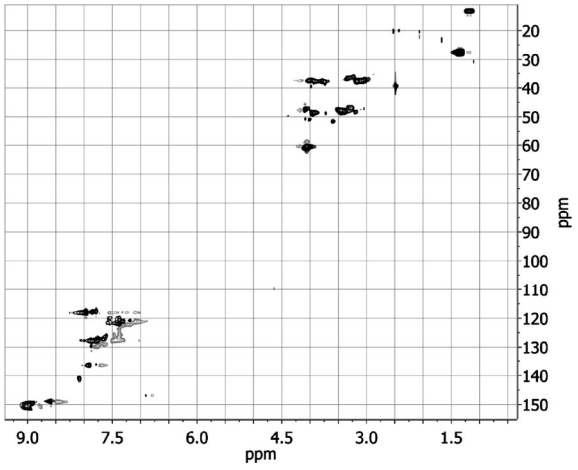

Figure 5. HMQC NMR spectra (400 MHz) of **7** in [D_6]DMSO.

complexes. Cyclic voltammetry was used to measure the formal potentials of these reactions for the dpt ligand and compounds **6** and **7**; the voltammograms are shown in Figure 6 and data summarized in Table 2. The dpt ligand has two sequential reduction waves at formal potentials of –2.00 and –2.40 V vs. SCE. Complexation of Pt causes an oxidative shift of the ligand-centered reductions by ca. 200 mV in **6** and **7**. In all cases the reduction reactions are chemically reversible with ΔE_p of 66–100 mV. For an electrochemically reversible system, according to the Nernst equation $\Delta E_p/n$ = 59 mV/n. Based on all of the observed values for ΔE_p, the reduction reactions are all one-electron processes (n = 1) and are reversible or nearly so.[24]

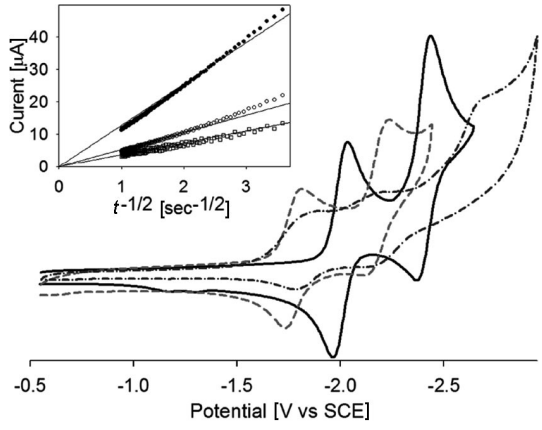

Figure 6. Cyclic voltammograms of DMF solutions containing 0.754 mM dpt ligand (–); 0.357 mM complex **6** (– –); and 1.535 mM complex **7** (– · –), and 0.2 M TBAP supporting electrolyte. Current is normalized for concentration. Potential scan rate was 50 mV/s. Inset: plots of the linearized current-time transients for the dpt ligand (●), complex **6** (○), complex **7** (□) resulting from applied potential steps to E = –2.25 V, –2.03 V, and –1.95 V for dpt, **6**, and **7**, respectively.

The diffusion coefficients D of each of the species are determined using potential-step chronoamperometry. The Figure 6 inset shows the linearized current (i) transients that are the result of applying potential steps to the mass-transport-limited region of the first reduction wave for each

Table 2. Electrochemical data for dpt and Pt(dpt) complexes.

	dpt	6	7
$E°$ [V][a]	–2.00	–1.79	–1.81
ΔE_p [mV][b]	66	80	78
$E°$ [V][a]	– 2.40	–2.19	–2.14
ΔE_p [mV][b]	66	100	64
E_a [V][c]			–2.62
$\Delta E°$ [V][d]	0.40	0.40	0.33
$D \times 10^5$ [cm^2/s][e]	2.87	1.88	1.55

[a] Formal potential measured as the average peak potential for the reaction in V vs. SCE. [b] Differences in the cathodic and anodic potentials in the cyclic voltammogram, measured at a potential scan rate of 50 mV/s. [c] Irreversible reduction peak. [d] Difference in formal potential of the first and second reduction reactions. [e] Diffusion coefficient calculated from the slopes of the Cottrell plots from chronoamperometry and analyzed using Equation (1).

molecule. The linearity of these plots indicates that each of these reduction reactions are diffusion controlled. The relationship between i and time (t) is described by the Cottrell equation (1).[24]

$$i = \frac{nFAD^{1/2}C}{\pi^{1/2}t^{1/2}} \quad (1)$$

where n is the number of electrons in the reaction (n = 1, based on analysis of the cyclic voltammograms); F is Faraday's constant, A is the surface area of the working electrode, and C is the concentration of the complex. These data were therefore used to calculate D for each species (Table 2). As expected, D decreases as the size of the redox active species increases,[25] but not drastically because the similarity in size for the structures.

Electronic Spectroscopy

Absorbance and emission spectra were recorded for all compounds and the summarized spectroscopic data are collected in Table 3. The absorbance spectra of **5**–**7** are very similar, and reveal only negligible shifts of the observed peaks. In each case the lowest energy absorption band is broad and appears between 360 and 434 nm, and has an extinction coefficient (ε) of ca. 1×10^4 M^{-1} cm^{-1} at the peak absorbance wavelength. This peak is assigned to the MLCT [d(Pt) – π*(dpt)] transition-based on its shape and intensity, although the extinction coefficient is higher than in related Pt(thpy)complexes (ε = 2000–6000 M^{-1} cm^{-1}).[8b,10c] The LC (π–π*) transition in compounds **6** and **7** is shifted to higher energy (326 to 328 nm) relative to this transition in uncoordinated dpt (340 nm). Coordination of the pyridyl ligands (in **6** and **7**) causes increased absorption at ca. 260 nm due to pyridine-centered π–π* transition.

In thoroughly dearated solutions, excitation of all three of the molecules at their MLCT maxima (λ_{ex} = 414 nm) gives rise to the emission spectra shown in Figure 7, which contain two peaks centered at 470 nm and at 640 nm. The latter of these is absent in the presence of oxygen. Structurally related [Pt(thpy)] complexes typically exhibit luminescence maxima around 550–570 nm in deaerated solutions.

Table 3. Summary of absorbance data and luminescence data.

	dpt	5	6	7
λ_{abs} [nm]	243 (5.5)	236 (16.6)	257 (18.9)	258 (21.4)
$\times 10^3$ ε	284 (7.6)	263 (15.1)	326 (28.9)	328 (27.0)
M^{-1} cm^{-1} [a]	340 (36.3)	323 (26.9)	413 (12.7)	415 (12.4)
	358[b] (24.4)	414 (12.7)	433[b] (10.5)	435[b] (10.2)
		432[b] (11.1)		
λ_{em} [nm][c]	390	470	470	470
k_F ($\times 10^6$) [s^{-1}][d]	19.3	0.91	1.1	0.24
k_{NR} ($\times 10^7$) [s^{-1}][e]	1.9	4.3	4.1	4.0
Φ_F[f]	0.44	0.023	0.027	0.006
λ_P [nm][c]		643, 704[j]	643, 704[j]	643, 704[j]
k_{ISC} ($\times 10^7$) [s^{-1}][g]		4.4	4.2	4.0
k_P ($\times 10^2$) [s^{-1}][h]		2.9	4.5	7.0
$k_{NR'}$ ($\times 10^5$) [s^{-1}][i]		1.4	1.5	2.3
Φ_P[f]		0.002	0.003	0.003

[a] Recorded in CH_3CN solutions at room temperature. [b] Shoulder. [c] Measured in degassed CH_3CN solution at room temperature. [d] $\tau_f = \left(\frac{1}{k_f + k_{nr}}\right)$. [e] $k_{nr} = \left(\frac{1-\Phi_F}{\tau_F}\right)$. [f] $\Phi_s = \Phi_r\left(\frac{\eta_s^2 A_r I_s}{\eta_r^2 A_s I_r}\right)$[9c]. [g] $\Phi_p = \left(\frac{k_{isc}}{k_f + k_{nr}}\right)\left(\frac{k_p}{k_p + k_{nr}}\right)$. [h] $\tau_p = \left(\frac{1}{k_p + k_{nr}}\right)$. [i] $k_{nr} = \left(\frac{1-\Phi_p}{\tau_p}\right)$. [j] Shoulder.

These have been attributed to relaxation of a ligand centered excited state [with some d-orbital mixing, d(Pt)-π*(C^N)], and with quantum yields of 0.01–0.31.[9b–9e,10b] In contrast, compounds **6** and **7** exhibit a higher energy emission peak that is observed even in the presence of oxygen, and with quantum yields (Φ_F) of 0.027 and 0.006 respectively. The lower energy emission peak (in deaerated solutions) has a lower quantum yield (Φ_P = 0.003).

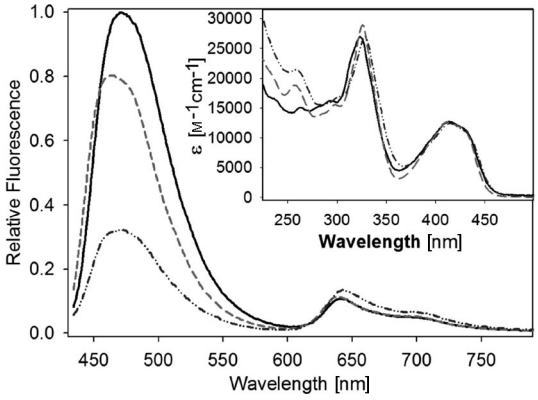

Figure 7. Emission spectra for compounds 12.6 μM **5** (–), 19.0 μM **6** (– –), and 7.2 μM **7** (–··–) in deaerated acetonitrile solutions following excitation at λ_{ex} = 414 nm. Spectra are normalized to concentration using known extinction coefficient. Inset: absorption spectra.

Time-resolved experiments were performed to determine the emission lifetimes of the photoexcited complexes, and these data indicate that the timescales for the higher and lower energy radiative relaxations differ greatly. The higher energy transitions have short lifetimes of 24 and 25 ns for **6** and **7**, respectively, whereas the lower energy transitions are relatively long lived (4.3–6.6 μs). This latter value is comparable to previously reported lifetimes for phosphorescence in Pt(thpy) complexes (0.7–19 μs).[9c,9d,10] On the basis of this, the differences lifetimes, and the quenching of the second peak in the presence of O_2,[27] we conclude that the two emissive peaks in the spectra for complexes **6** and **7** are fluorescence (high energy) and phosphorescence (low energy) transitions.

Using the quantum yield and lifetimes, these data were used to determine the rates of radiative decay for each of the molecules; in Table 3, the rates of non-radiative decay (k_{NR}) are nearly the same for all of the Pt complexes. Values for the higher energy fluorescence peak range from 0.240–1.125 $\times 10^6$ s^{-1}, which are consistent with a fluorescent transition (k_F).[26] Conversely, the much slower rates of radiative decay for the lower energy transition (i.e. at 640 nm) of complexes **6** and **7** is consistent with phosphorescence. Using the rates of emission for the fluorescent and phosphorescent transitions (k_F and k_P), the rate of inter-system crossing (k_{ISC}) was determined to be on the same timescale as non-radiative relaxation (k_{NR}). The similarity of these data for the two Pt complexes implies that the aeg backbone does not play a role in the photochemistry of these molecules. Therefore, the Pt-containing pyridine dipeptide is a fluorescent and phosphorescent complex that can be employed as an emissive label in synthetic peptides.

Conclusions

We have synthesized a pyridine-substituted artificial dipeptide, and used the two ligands to form a [Pt(dpt)-$(py)_2$]$^{1+}$ complex on the aeg scaffold. X-ray structural characterization of a small molecule analog, together with extensive NMR spectroscopy, is used to determine the structure of the metallated dipeptide. The monometallic dipeptide complex has reversible reductive electrochemically, and is both luminescent and fluorescent. Continuing efforts seek to employ the Pt(dpt) dipeptide as a substitutionally inert fluorescent tag in artificial peptide sequences.

Experimental Section

Chemicals: K_2PtCl_4 was purchased from Strem and 2-ethynylpyridine was purchased from GFS Chemicals, Inc. (GFS). All other

materials were purchased from either Sigma–Aldrich or VWR and used as received unless otherwise noted. Dichloromethane and tetrahydrofuran (thf) were dried on an activated alumina column. For all experiments, ultrapure water was used (Labconco Water Pro PS system, 18.2 MΩ).

Instrumentation and Analysis: Positive-ion electrospray mass spectrometry (ESI+) was performed at the Penn State Mass Spectrometry Facility using a Mariner mass spectrometer (Perseptive Biosystems.) ^{1}H, ^{13}C, COSY, HMBC, and HMQC NMR spectra were collected with a 400 MHz spectrometer (Bruker); variable-temperature spectra were collected on a 300-MHz spectrometer (Bruker).

The UV/Vis absorbance spectra were obtained with a double-beam spectrophotometer (Varian, Cary 500) using a 1-cm quartz cuvette in HPLC-grade acetonitrile. Steady-state emission experiments were performed using a 1-cm quartz cuvette at room temperature by a PTI Photon Technology Instruments using an 814 photomultiplier detection system. Lifetime measurements were monitored following excitation from a PTI Nitrogen laser GL-302 Dye Laser with PBBO laser dye and a 50 μs collection time per point. Quantum efficiency measurements were carried out in room temperature in HPLC grade acetonitrile. Samples were measured in both aerated and deaerated solutions following literature methods.[9c] Solutions of deaerated $Ru(bpy)_3^{2+}$ (Φ = 0.062) in acetonitrile and anthracene (Φ = 0.27) in ethanol were used as references.

Electrochemistry: All electrochemical measurements were obtained using a CH Instruments potentiostat (Model 660) with a 0.31-cm diameter glassy-carbon working and Pt wire counter electrodes with a Ag/Ag^+ reference electrode. Solutions were prepared from distilled DMF containing 0.2 M tetra-*n*-butylammonium perchlorate (TBAP, recrystallized three times) supporting electrolyte. The solutions were prepared, stored, and analyzed in an N_2-saturated environment. The redox potentials are based on cyclic voltammograms and are reported relative to a ferrocene/ferrocenium (Cp_2Fe/Cp_2Fe^+) redox couple used as an internal reference.[24] Chronoamperometric measurements were corrected for background currents by subtracting the current transients obtained from potential steps of equal magnitude applied in solutions containing solely supporting electrolyte.

X-ray Crystallography: An orange rod-shaped crystal of the dpt ligand and a yellow plate-shaped crystal of **6** were coated in paratone freezing oil, picked up with nylon loops and mounted in the nitrogen cold stream of the diffractometer. X-ray intensity data were measured at 126(2) K, cooled by a Rigaku-MSC X-Stream 2000 and at 298(2) K for the dpt ligand and **6**, respectively. The intensity data was collected with a Bruker SMART APEX CCD area detector system equipped with a graphite monochromator and a Mo-K_α fine-focus sealed tube (λ = 0.71073 Å) operated at 1600 W power. Data reduction (including intensity integration, background, Lorentz and polarization corrections) was performed by use of the Bruker software package. The structure was solved by direct methods (SHELXS)[28] and refined by the full-matrix, least-squares method based on F^2 against all reflections (SHELXL).[29] All non-hydrogen atoms were refined anisotropically. Hydrogen atoms were placed geometrically and were refined by use of the riding model. Crystallographic data of dpt and **6** are listed in Table 4.

CCDC-689631 (for dpt) and -689632 (for **6**) contain the supplementary crystallographic data. These data can be obtained free of charge from The Cambridge Crystallographic Data Centre via www.ccdc.cam.ac.uk/data_request/cif.

Synthesis: *Caution: Perchlorate salts are potentially explosive and should be handled with care.*

Table 4. Crystal data and structure refinement for dpt and $Pt(dpt)(4\text{-pic})_2$ (**6**).

	dpt	$Pt(dpt)(4\text{-pic})_2$ (**6**)
Empirical formula	$C_{14}H_{10}N_2S$	$C_{26}H_{23}N_4PtS$
Fw	238.30	702.08
T [K]	126(2)	298(2)
λ [Å]	0.71073	0.71073
Crystal system	orthorhombic	triclinic
Space group	*P*2(1)2(1)2(1)	$P\bar{1}$
Crystal size [mm]	0.49 × 0.12 × 0.10	0.18 × 0.15 × 0.06
a [Å]	5.809	9.7243
b [Å]	14.321	11.9387
c [Å]	14.321	12.7757
α [deg]	90	68.238
β [deg]	90	83.007
γ [deg]	90	83.833
V [Å^3]	1184.4	1364.1
Z	4	2
ρ_{calc} [g cm^{-3}]	1.336	1.709
μ [mm^{-1}]	0.249	5.351
Final R_1 (obsd. data)[a]	0.0353	0.0508
Final wR_2 (all data)[b]	0.0845	0.1337

[a] $R_1 = \Sigma||F_o| - |F_c||/\Sigma|F_o|$. [b] $wR_2 = [\Sigma[w(F_o^2 - F_c^2)^2]/\Sigma[w(F_o^2)_2]]^{1/2}$, where $w = 1/\sigma^2(F_o^2) + (aP)^2 + bP$, $P = (F_o^2 + 2F_c^2)/3$.

N-*tert*-Butoxycarbonyl-1,2-diaminoethane (boc-en),[30] ethyl *N*-[(2-Boc-amino)ethyl]glycinate (Boc-aeg-OEt),[31] 2,5-bis(2-pyridyl)-thiophene (dpt),[32] and diiodo(cycloocta-1,5-diene)platinum(II)[33] were synthesized as previously reported.

Ethyl {*N*-[2-(*tert*-Butoxycarbonylamino)ethyl]-*N*-[2-(4-pyridyl)-acetyl]amino}acetate [Boc-(py-aeg)-OEt]: Using a procedure adapted from the literature,[34] a suspension of 4-pyridylacetic acid hydrochloride (0.83 g, 4.8 mmol), dicyclohexylcarbodiamide (DCC) (0.898 g, 4.4 mmol), and 4-(dimethylamino)pyridine (DMAP) (0.053 g, 0.44 mmol) in 50 mL of dry dichloromethane was stirred for 15 min at 0 °C. To this was added *N*-methylmorpholine (NMM) (1.07 mL, 17.4 mmol), and the mixture stirred for an additional 15 min. The reaction solution was then added to Boc-aeg-OEt (1.07 g, 4.4 mmol) in dry dichloromethane (75 mL), and the solution stirred for 48 h at room temperature. Following extraction with water (3 × 50 mL), the dichloromethane layer was dried with sodium sulfate, filtered, and reduced in volume to 10 mL. The product was purified on silica using a gradient (ethyl acetate to 10% methanol in ethyl acetate); collected fractions were dried under vacuum to give 0.9431 g of a yellow oil (59% yield). ^{1}H NMR (400 MHz, $CDCl_3$): δ = 1.24 (t, 3 H), 1.39 (d, 9 H), 3.23 (dd, 2 H), 3.47 (dd, 2 H), 3.72 (s, 2 H), 3.98 (s, 2 H), 4.17 (dt, 2 H), 7.16 (m, 2 H), 8.50 (dd, 2 H) ppm.

{*N*-[2-(*tert*-Butoxycarbonylamino)ethyl]-*N*-[2-(4-pyridyl)acetyl]-amino}acetic Acid (2): This synthesis was adapted from a published procedure.[35] Boc-(py-aeg)-OEt (1.82 g, 5.0 mmol) was suspended in thf (13 mL) and cooled to 0 °C. 1 M NaOH (8 mL) was added, and the solution was stirred overnight and warmed to room temperature. The reaction mixture was subsequently filtered, 25 mL of water was added, and the solution extracted with dichloromethane (2 × 25 mL). After adjusting the pH of the aqueous solution to 2.0 with 1 M aqueous HCl, the solvent was removed under vacuum to yield a yellow-white powder. The solid was dissolved in 10 mL methanol, filtered, and the solvent removed under vacuum yielding 1.09 g (64.8%) of yellow foam. ^{1}H NMR (400 MHz, $[D_3]$MeOH): δ = 1.25 (d, 9 H), 3.10 (dd, 2 H), 3.38 (m, 2 H), 3.94 (s, 2 H), 4.16 (s, 2 H), 7.88 (dd, 1 H), 8.20 (d, 1 H), 8.59 (d, 1 H), 8.67 (t, 1 H) ppm.

Ethyl {*N*-(2-Aminoethyl)-*N*-[2-(4-pyridyl)acetyl]amino}acetate: This synthesis was modified based on a literature procedure;[36] briefly, Boc-(py-aeg)-OEt (0.88 g, 2.4 mmol) was stirred for 1 h at 0 °C in a mixture of methanol (10 mL), water (10 mL), and concentrated aqueous HCl (10 mL). After removing the solvent under vacuum, the remaining yellow residue was dissolved in dichloromethane (20 mL) and extracted with water (3 × 15 mL). The aqueous layer was reduced under vacuum to give 0.482 g of yellow foam (75.4% yield). ^{1}H NMR (400 MHz, [D$_3$]MeOH): δ = 1.26 (m, 3 H), 3.19 (t, 2 H), 3.79 (t, 2 H), 4.20 (s, 2 H), 4.46 (m, 2 H), 8.09 (dd, 2 H), 8.82 (m, 2 H) ppm.

Boc-(py-aeg)$_2$-OEt (4): A suspension of **2** (1.67 g, 4.9 mmol), *o*-benzotriazolyl-*N*,*N*,*N*′,*N*′-tetramethyl-uronium hexafluorophosphate (HBTU) (1.10 g, 2.9 mmol), and *N*-hydroxybenzotriazole (HOBt) (0.44 g, 2.9 mmol) in 50 mL of dry dichloromethane was stirred for 15 min at 0 °C. To this was added diisopropylethylamine (DIPEA) (2.02 mL, 11.6 mmol), and the mixture was stirred for an additional 15 min. This mixture was added to a solution of **3** (0.77 g, 2.9 mmol) in dry dichloromethane (75 mL) and stirred for 72 h at room temperature. The solution was extracted with water (3 × 50 mL) and dried with sodium sulfate. The volume of the solution was reduced to 10 mL, and the remaining solution chromatographed on silica using a gradient (ethyl acetate to 50% methanol in ethyl acetate). The column progress was monitored by thin-layer chromatography in ethyl acetate/methanol (50:50), collecting the second major band (R_f = 0.5). The resulting solution was dried under vacuum yielding a yellow oil 0.590 g (34.8% yield). (ESI +) calculated: [M + H]$^+$ = 585.3, [M + Na]$^+$ = 607.3; found [M + H]$^+$ = 585.2, [M + Na]$^+$ = 607.3. ^{1}H NMR (400 MHz, [D]CDCl$_3$): δ = 1.15 (dt, 3 H), 1.34 (s, 9 H), 3.1–3.5 (m, 10 H), 3.6–3.78 (m, 4 H), 3.97 (d, 2 H), 4.10 (dd, 2 H), 7.09 (m, 4 H), 8.38 (m, 4 H) ppm.

Bis(acetonitrile)(2,5′dipyridylthiophene)platinum(II) Perchlorate [Pt(dpt)(ACN)$_2$]ClO$_4$ (5): Complex **5** was prepared using a slightly modified literature method;[18] silver perchlorate (186 mg, 0.89 mmol) was added to a suspension of diiodo(cycloocta-1,5-diene)platinum(II) (250 mg, 0.45 mmol) in acetone (5 mL). The mixture was stirred until the solution was clear and colorless; AgI precipitated and was centrifuged. The solution was then decanted and added to a solution of dpt (100 mg, 0.42 mmol) in acetonitrile (5 mL) and the reaction mixture refluxed for 24 h. The resulting precipitate was collected by centrifugation, washed with diethyl ether and dried under vacuum. The crude product was further purified using silica column chromatography by eluting with acetonitrile/water: saturated potassium nitrate (5:4:1) and the second band (monitored by thin layer chromatography) was collected and like fractions combined. The resulting product was reduced under vacuum yielding 136.6 mg (53% yield) of the yellow Pt complex. (ESI +) calculated: (M$^+$ no ACN) = 432.01, (M$^+$ + ACN) = 473.04; found (M$^+$ no ACN) = 432.2, (M$^+$ + ACN) = 473.2. ^{1}H NMR (400 MHz, [D$_6$]DMSO): δ = 7.37 (t, 1 H), 7.42 (t, 1 H), 7.63 (s, 1 H), 7.82 (d, 1 H), 7.88 (t, 1 H), 8.03–8.18 (m 2 H), 8.53 (d, 2 H) ppm.

[Pt(dpt)(4-pic)$_2$]NO$_3$ (6): Complex **6** was prepared by reacting complex **5** (138 mg, 0.23 mmol) with 4-picoline (44 μL, 0.45 mmol) in acetonitrile (5 mL) at room temperature for 3 d. Addition of diethyl ether precipitated the crude Pt^{II} complex, which was further purified using silica column chromatography by eluting with acetonitrile/water: saturated potassium nitrate (5:4:1). The second band (monitored by thin layer chromatography) was collected and like fractions combined. The resulting product was isolated by slow evaporation of the solution, yielding 93.6 mg (61% yield) of crystalline product. (HR ESI+) Calculated: [M$^+$] = 617.1270; found [M$^+$] = 617.1281. ^{1}H NMR (400 MHz, [D$_6$]DMSO): δ = 2.44 (d, 2 H), 6.81 (s, 1 H), 7.12 (t, 1 H), 7.29 (t, 1 H), 7.50 (d, 3 H), 7.58 (d, 2 H), 7.77 (m, 3 H), 8.04 (t, 1 H), 8.52 (d, 1 H), 8.88 (t, 4 H) ppm. Further confirmation of purity and identity were accomplished with COSY, HMQC and HMBC NMR as described below.

[Pt(dpt)(py-aeg)$_2$] Dipeptide (7): Complex **7** was prepared by reacting 209 mg complex **5** (0.34 mmol) with complex **4** (192 mg, 0.33 mmol) in acetonitrile (5 mL) and stirring at room temperature for 3 d. The resulting complex was precipitated by addition of diethyl ether to give the crude Pt^{II} complex which was purified by silica column chromotagraphy using acetonitrile/water/saturated potassium nitrate (5:4:1) as the mobile phase. The second band (monitored by thin-layer chromatography) was collected and like fractions combined. Resulting product was isolated by extraction with dichloromethane (3 × 20 mL). This solution was dried with sodium sulfate and volume reduced under vacuum. The resulting yellow precipitate was isolated by dissolving in acetonitrile and precipitation with diethyl ether solution yielding 170 mg (44.5% yield). (ESI+) Calculated: [M$^+$] = 1061.3; found [M$^+$] = 1016.2. ^{1}H NMR (400 MHz, [D$_6$]DMSO): δ = 7.13 (m, 1 H), 7.27 (m, 1 H), 7.47–7.54 (m, 4 H), 7.75 (m, 2 H), 7.78–7.89 (m, 2 H), 8.03 (t, 1 H), 8.54 (d, 1 H), 8.83–8.94 (m, 4 H) ppm. Further confirmation of purity and identity were accomplished with COSY and HMQC NMR (see Supporting Information).

Supporting Information (see also the footnote on the first page of this article): Example NMR spectra, including ^{1}H, ^{13}C, COSY, HMBC, and HMQC spectra as well as ESI-TOF mass spectrometric spectra and time-resolved emission spectra.

Acknowledgments

We gratefully acknowledge financial support of this work by a Packard Fellowship for Science and Engineering and a grant from the National Science Foundation (NSF) (CHE-0718373). The X-ray crystallography facility is supported by a grant from the National Science Foundation (CHE-0131112). We thank C. Morgan and J. Youngblood for helpful discussions.

[1] a) L. A. Levine, C. M. Morgan, K. Ohr, M. E. Williams, *J. Am. Chem. Soc.* **2005**, *127*, 16764–16765; b) A. Mokhir, R. Krämer, H. Wolf, *J. Am. Chem. Soc.* **2004**, *126*, 6208–6209.

[2] a) B. P. Gilmartin, K. Ohr, R. L. McLaughlin, R. Koerner, M. E. Williams, *J. Am. Chem. Soc.* **2005**, *127*, 9546–9555; b) K. Ohr, B. P. Gilmartin, M. E. Williams, *Inorg. Chem.* **2005**, *44*, 7876–7885; c) B. P. Gilmartin, R. L. McLaughlin, M. E. Williams, *Chem. Mater.* **2005**, *17*, 5446–5454; d) K. Ohr, R. L. McLaughlin, M. E. Williams, *Inorg. Chem.* **2007**, *46*, 965–974; e) S. I. Kirin, H. P. Yennawar, M. E. Williams, *Eur. J. Inorg. Chem.* **2007**, 3686–3694.

[3] a) A. Küsel, J. Zhang, M. A. Gil, A. C. Stückl, W. Meyer-Klaucke, F. Meyer, U. Diederichsen, *Eur. J. Inorg. Chem.* **2005**, 4317–4324; b) J. Brasún, P. Ciapetti, H. Kozlowski, S. Oldziej, M. Taddei, D. Valensin, G. Valensin, N. Gaggelli, *J. Chem. Soc., Dalton Trans.* **2000**, 2639–2644; c) D.-L. Popescu, T. J. Parolin, C. Achim, *J. Am. Chem. Soc.* **2003**, *125*, 6354–6355; d) R. M. Watson, Y. A. Skorik, G. K. Patra, C. Achim, *J. Am. Chem. Soc.* **2005**, *127*, 14628–14639; e) R. M. Franzini, R. M. Watson, G. K. Patra, R. M. Breece, D. L. Tierney, M. P. Hendrich, C. Achim, *Inorg. Chem.* **2006**, *45*, 9798–9811.

[4] A. Mokhir, R. Stiebing, R. Kraemer, *Bioorg. Med. Chem. Lett.* **2003**, *13*, 1399–1401.

[5] C. P. Myers, B. P. Gilmartin, M. E. Williams, *Inorg. Chem.* **2008**, *47*, 6738–6747.

[6] L. Zhang, E. Meggers, *J. Am. Chem. Soc.* **2005**, *127*, 74–75.
[7] J. C. Verheijen, G. A. van der Marel, J. H. van Boom, N. Metzler-Nolte, *Bioconjugate Chem.* **2000**, *11*, 741–743.
[8] a) L. Chassot, E. Müller, A. von Zelewsky, *Inorg. Chem.* **1984**, *23*, 4249–4253; b) L. Chassot, A. von Zelewsky, *Inorg. Chem.* **1987**, *26*, 2814–2818.
[9] a) P.-I. Kvam, J. Songstad, *Acta Chem. Scand.* **1995**, *49*, 313–324; b) P.-I. Kvam, M. V. Puzyk, V. S. Cotlyr, K. P. Balashev, J. Songstad, *Acta Chem. Scand.* **1995**, *49*, 645–652; c) J. Brooks, Y. Babayan, S. Lamansky, P. I. Djurovich, I. Tsyba, R. Bau, M. E. Thompson, *Inorg. Chem.* **2002**, *41*, 3055–3066; d) W. Lu, M. C. W. Chan, N. Zhu, C.-M. Che, C. Li, Z. Hui, *J. Am. Chem. Soc.* **2004**, *126*, 7639–7651; e) S. W. Thomas III, K. Venkatesan, P. Müller, T. M. Swager, *J. Am. Chem. Soc.* **2006**, *128*, 16641–16641; f) P. I. Djurovich, D. Murphy, M. E. Thompson, B. Hernandez, R. Gao, P. L. Hunt, M. Selke, *Dalton Trans.* **2007**, 3763–3770.
[10] a) D. Sandrini, M. Maestri, V. Balzani, L. Chassot, A. von Zelewsky, *J. Am. Chem. Soc.* **1987**, *109*, 7720; b) K. P. Balashev, M. V. Puzyk, V. S. Kotlyar, M. V. Kulikova, *Coord. Chem. Rev.* **1997**, *159*, 109–120; c) K. P. Balashev, M. A. Ivanov, T. V. Taraskina, E. A. Cherezova, *Russ. J. Gen. Chem.* **2006**, *76*, 781–790.
[11] a) S. Lamansky, R. C. Kwong, M. Nugent, P. I. Djurovich, M. E. Thompson, *Org. Electron.* **2001**, *2*, 53–62; b) Y.-Y. Lin, S.-C. Chan, M. C. W. Chan, Y.-J. Hou, N. Zhu, C.-M. Che, Y. Liu, Y. Wang, *Chem. Eur. J.* **2003**, *9*, 1264–1272; c) M. Cocchi, D. Virgili, C. Sabatini, V. Fattori, P. Di Marco, M. Maestri, J. Kalinowski, *Synth. Met.* **2004**, *147*, 253–256; d) B. Ma, P. I. Djurovich, M. E. Thompson, *Coord. Chem. Rev.* **2005**, *249*, 1501–1510; e) G.-J. Zhou, X.-Z. Wang, W.-Y. Wong, X.-M. Yu, H.-S. Kwok, Z. Lin, *J. Organomet. Chem.* **2007**, *692*, 3461–3473; f) G. D. Batema, M. Lutz, A. L. Spek, C. A. van Walree, C. de Mello Donegá, A. Meijerink, R. W. A. Havenith, J. Pérez-Moreno, K. Clays, M. Büchel, A. van Dijken, D. L. Bryce, G. P. M. van Klink, G. van Koten, *Organometallics* **2008**, *27*, 1690–1701.
[12] a) R. Palmans, A. J. Frank, *J. Phys. Chem.* **1991**, *95*, 9438–9443; b) T. Maruyama, T. Yamamoto, *J. Phys. Chem. B* **1997**, *101*, 3806–3810; c) K. Sakai, H. Ozawa, *Coord. Chem. Rev.* **2007**, *251*, 2753–2766.
[13] a) S. S. Kamath, S. Shukla, T. S. Srivastava, *Bull. Chem. Soc. Jpn.* **1991**, *64*, 1351–1358; b) X.-H. Li, L. Z. Wu, L.-P. Zhang, C.-H. Tung, C.-M. Che, *Chem. Commun.* **2001**, 2280–2281; c) N. M. Shavaleev, H. Adams, J. Best, R. Edge, S. Navaratnam, J. A. Weinstein, *Inorg. Chem.* **2006**, *45*, 9410–9415.
[14] a) M. Hissler, J. E. McGarrah, W. B. Connick, D. K. Geiger, S. D. Cummings, R. Eisenberg, *Coord. Chem. Rev.* **2000**, *208*, 115–137; b) A. Islam, H. Sugihara, K. Hara, L. P. Singh, R. Katoh, M. Yanagida, Y. Takahashi, S. Murata, H. Arakawa, *Inorg. Chem.* **2001**, *40*, 5371–5380; c) S. Chakraborty, T. J. Wadas, H. Hester, R. Schmehl, R. Eisenberg, *Inorg. Chem.* **2005**, *44*, 6665–6678.
[15] a) A. H. J. Wang, J. Nathan, G. van der Marel, J. H. van der Boom, A. Rich, *Nature* **1978**, *276*, 471–474; b) C. S. Peyratout, T. K. Aldridge, D. K. Crites, D. R. McMillin, *Inorg. Chem.* **1995**, *34*, 4484–4489; c) H.-Q. Liu, T.-C. Cheung, C.-M. Che, *Chem. Commun.* **1996**, 1039–1040; d) C.-M. Che, M. Yang, K.-H. Wong, H.-L. Chan, W. Lam, *Chem. Eur. J.* **1999**, *5*, 3350–3356; e) D.-L. Ma, C.-M. Che, *Chem. Eur. J.* **2003**, *9*, 6133–6144; f) P. K.-M. Siu, D.-L. Ma, C.-M. Che, *Chem. Commun.* **2005**, 1025–1027.
[16] a) G. W. V. Cave, F. P. Fanizzi, R. J. Deeth, W. Errington, J. P. Rourke, *Organometallics* **2000**, *19*, 1355–1364; b) C. P. Newman, G. W. V. Cave, M. Wong, W. Errington, N. W. Alcock, J. P. Rourke, *J. Chem. Soc., Dalton Trans.* **2001**, 2678–2682; c) W. Lu, N. Zhu, C.-M. Che, *Chem. Commun.* **2002**, 900–901.
[17] a) E. Meggers, P. L. Holland, W. B. Tolman, F. E. Romesberg, P. G. Schultz, *J. Am. Chem. Soc.* **2000**, *122*, 10714–10715; b) S. Atwell, E. Meggers, G. Spraggon, P. G. Schultz, *J. Am. Chem. Soc.* **2001**, *123*, 12364–12367; c) N. Zimmerman, E. Meggers, P. G. Schultz, *Bioorg. Chem.* **2004**, *32*, 13–25; d) K. Tanaka, G. H. Clever, Y. Takezawa, Y. Yamada, C. Kaul, M. Shionoya, T. Carell, *Nat. Nanotechnol.* **2006**, *1*, 190–194; e) K. Tanaka, M. Shionoya, *Coord. Chem. Rev.* **2007**, *251*, 2732–2742.
[18] G. Lowe, T. Vilaivan, *J. Chem. Res. (S)* **1996**, 386–387.
[19] J. Breu, K.-J. Range, A. von Zelewsky, H. Yersin, *Acta Crystallogr., Sect. C* **1997**, *53*, 562–565.
[20] a) A. C. Stückl, U. Klement, K.-J. Z. Range, *Kristallogr.* **1993**, *208*, 297–298; b) T. J. Giordano, P. G. Rasmussen, *Inorg. Chem.* **1975**, *14*, 1628–1634.
[21] M. Ghedini, D. Pucci, A. Crispini, G. Barberio, *Organometallics* **1999**, *18*, 2116–2124.
[22] R. L. McLaughlin, *The Pennsylvania State University*, **2005**, Honors thesis in Chemistry.
[23] For example: a) M. Oleszczuk, S. Rodziewicz-Motowidlo, B. Falkiewicz, *Nucleosides Nucleotides Nucleic Acids* **2001**, *20*, 1399; b) S. M. Chen, V. Mohan, J. S. Kiely, M. C. Griffith, R. H. Griffey, *Tetrahedron Lett.* **1994**, *35*, 5105–5108.
[24] A. J. Bard, L. R. Faulkner, *Electrochemical Methods, Fundamentals and Applications*, 2nd ed., John Wiley & Sons, New York, **2001**.
[25] P. Atkins, J. de Paula, *Physical Chemistry*, 7th ed., W. H. Freeman and Company, New York, **2002**.
[26] J. D. Ingle Jr., S. R. Crouch, *Spectrochemical Analysis*; Prentice-Hall, New Jersey, **1988**.
[27] D. A. Andreeva, M. V. Puzyk, *Opt. Spectrosc.* **2003**, *95*, 714–714.
[28] G. M. Sheldrick, *SHELXS97*, Program for the Solution of Crystal Structures, University of Göttingen, Germany, **1997**.
[29] G. M. Sheldrick, *SHELXL97*, Program for the Refinement of Crystal Structures, University of Göttingen, Germany, **1997**.
[30] A. P. Krapcho, C. S. Kuell, *Synth. Commun.* **1990**, *20*, 2559–2564.
[31] G. Breipohl, D. W. Will, A. Peyman, E. Uhlmann, *Tetrahedron* **1997**, *53*, 14671–14686.
[32] a) S. A. Al-Taweel, *Phosphorus Sulfur Silicon* **2002**, *177*, 1041–1045; b) K. Takahashi, T. Nihira, *Bull. Chem. Soc. Jpn.* **1992**, *65*, 1855–1859.
[33] J. X. McDermott, J. F. White, G. M. Whitesides, *J. Am. Chem. Soc.* **1976**, *98*, 6521–6528.
[34] S. I. Kirin, K. Ohr, H. P. Yennawar, C. M. Morgan, L. A. Levine, M. E. Williams, *Inorg. Chem. Commun.* **2007**, *10*, 652–656.
[35] K. L. Dueholm, M. Egholm, C. Behrens, L. Christensen, H. F. Hansen, T. Vulpius, K. H. Petersen, R. H. Berg, P. E. Nielsen, O. Buchardt, *J. Org. Chem.* **1994**, *59*, 5767–5773.
[36] Y. Qu, H. Rauter, A. P. S. Fontes, R. Bandarage, L. R. Kelland, N. Farrell, *J. Med. Chem.* **2000**, *43*, 3189–3192.

Received: June 11, 2008
Published Online: August 8, 2008

